Published in Composites Science and Technology 2014, Vol 94, pp. 123-131

Experimental characterisation of mixed mode traction-displacement relationships for a single carbon composite Z-pin

M. Yasaee[1], J.K. Lander[2], G. Allegri and S. R. Hallett

Advanced Composites Centre for Innovation and Science (ACCIS), University of Bristol, Queen's Building, University Walk, Bristol, BS8 1TR, UK

Abstract

This paper presents an experimental characterisation of the mechanical performance and behaviour of through-thickness reinforced composite laminates. To achieve this, composite blocks with individual reinforcing pins were manufactured, quality assessed and tested. Individual specimens were inspected using X-ray Computed Tomography and only the specimens with acceptable quality pin insertions were tested experimentally under a range of mode mixities. Two stacking sequences, uni-directional (UD) and quasi-isotropic (QI) were investigated. It was found that the pins inside the UD samples experienced significantly larger pin/matrix bond strength than those in the QI laminates. The resulting experimental data indicates that a non-UD laminate type may experience pin pull-out and thus increased energy absorption for a wider range of mode mixities than a UD laminate type. Energy plots show a clear transition from a pull-out to a pin rupture region for both laminate types. Specimens that experienced pin rupture during low mode mixity tests exhibited similar failure energies to those loaded in pure mode II.

Keywords: A. Structural composites, B. Delamination, C. Damage Mechanics, C. Fibre Bridging, D. Z-Pinning

[1] Corresponding author: m.yasaee@bristol.ac.uk; +44(0) 117 33 15098
[2] Present address: Rolls-Royce Plc, PO Box 31, Moor Lane, Derby, DE24 8BJ

1. Introduction

The lack of reinforcement in the thickness direction of laminated composites leads to delamination damage as the dominant failure mode in many practical applications. Techniques developed to reinforce laminated composite in the thickness direction include stitching [1], tufting and Z-pinning [2]. Z-pinning is a process whereby small diameter pins, made from fibrous composites or metals, are inserted through the thickness (Z-axis direction) of the composite material. This reinforcement process is performed prior to final cure and results in a composite structure with increased resistance to delamination growth [3], thus improving impact damage tolerance [4]. They can also be used to join structural composite parts, such as T-stiffners [5,6].

Experimental studies on Z-pinned composite laminates have typically characterised arrays of pins through standard fracture toughness tests [5,7] and bespoke pull-out and shear tests [7–9]. However, due to the pin-to-pin interaction and to the large variation of the inserted pin quality and misalignment angles which arise from the manufacturing process [10], it is difficult to extract single pin behaviour from such tests and the final orientation of individual pins relative to the loading direction will be incidental rather than desired. Cartié *et al.* [11] investigated the crack bridging mechanism of single carbon composite and metallic pins in the mode I and mode II loading regimes. In mode I the pins pull-out of the composite block. The response includes debonding of the pin with surrounding matrix followed by a phase dominated by pin/matrix friction. In mode II it was shown that the pin orientation relative to the mode II loading direction determines the bridging mechanism. When loading direction is “with the nap” (Figure 1 a) the pin will exhibit a pull-out response whereas when loaded “against the nap” (Figure 1 b) the pin fails in bending or shear, exhibiting brittle behaviour. However, it is important to note that the fixture used for

the mode II experiment of the carbon composite pins was not laterally constrained, thereby allowing opening displacements during the test and hence the failure mechanism cannot be regarded as pure mode II.

(*Insert figure 1*)

More recently Mouritz and Koh [9] have made new evaluations of the bridging mode I tractions definitions. Experiments on the mode I traction loads of 49 pins inserted in a 10mm square array for varying composite thicknesses were carried out. A tri-linear mode I bridging traction curve was defined to describe the response they observed.

The majority of fracture toughness and the single or multiple pin array experimental tests have been carried out using standard uni-directional (UD) laminates which are not typical of layups used in practical engineering applications. Sweeting *et al.* [12] used finite element (FE) modelling to investigate the generation of thermal residual stresses around the pins which arise during the curing cycle, due to thermal expansion coefficient mismatch between the pins and a cross-ply composite substrate. This raises the question of whether stacking sequences will strongly influence a pin's bridging mechanism, and thus the effectiveness of its performance.

The purpose of the current investigation was to characterise the bridging mechanisms of a single carbon composite pin inserted through the thickness of a composite block. Bespoke testing fixtures were manufactured to provide mode I, mode II and mixed mode loading cases. Specimens were manufactured using two stacking sequences, uni-directional and quasi-isotropic (QI) and the influence on the pin response analysed.

Approaches to describe the through thickness reinforced (TTR) pin bridging mechanisms analytically have been attempted by a number of [13–17]. In all these

cases the TTR bridging models have been calibrated against experimental data carried out either on mode I pin array pull-out tests [16], standard mode I fracture toughness tests [7], T-Joint pull-out tests [2,5,6,15] or mode I and mode II single pin tests [11,14]. However, no single, complete set of data on a wide range of mode mixities and in different stacking sequences exists. The single pin response data generated in this investigation is an essential requirement for the effective development and calibration of pin bridging laws implemented into cohesive zone models for high fidelity finite element analyses.

2. Specimen Manufacture

A schematic diagram of a pinned specimen manufactured for this investigation is shown in Figure 2. Each specimen was manufactured from 64 plies of IM7/8552 prepreg (Hexcel, UK) with a 16μm thick PTFE release film inserted at the mid-plane, giving a nominal total specimen thickness of 8mm. The PTFE film was used to ensure that the two halves of the specimen were not bonded, allowing only the pin bridging forces to be measured. The insertion of a single 0.28mm diameter T300 carbon/BMI pin through the thickness was performed manually after warming uncured laminate on a hot plate i.e. gently pressing the pin through a warmed laminate. Manual insertion was adopted to give greater control of the final state of the pins. Readers must note that this will not be a precise representation of the UAZ insertion process, but it is believed that a pin of the same inclination and insertion quality will behave in much the same manner, regardless of manufacturing method. The stacking sequences for the UD samples were $[0_{32}/10 // 0_{32}]$. The additional 10° ply was added at the mid-plane to prevent the interpenetration or ‘nestling’ of the fibres across the mid-plane which

would interlock and cause traction forces over and above those exerted by the pin, or induce opening of the specimen, especially when loaded with high mode II mixities.

The QI laminate stacking sequence $[(0/45/90/-45)_{4s}//\ (90/-45/0/45)_{4s}]$ was designed such that there was a 0/90 interface at the centre-line to avoid fibre nestling. The top and bottom halves of the specimen were balanced and symmetric and the asymmetry in the total specimen stacking sequence was sufficiently small so as not to cause any significant deformation of the cured laminate.

(*Insert figure 2*)

Each specimen was carefully machined from a composite plate (Figure 2a). The arrangement of the release film was such that specimens could be cut ensuring that there was an additional length of 5mm that remained bonded (Figure 2b) across the mid plane. This extra bonded length supported the pin/laminate interface and allowed safe handling during machining and X-ray Computed Tomography (CT) inspection. The extra bonded length was machined off immediately prior to testing to the dimensions shown in Figure 2c, taking care not to displace or rotate the de-bonded top and bottom blocks and damage the pin/laminate interface.

3. Pin misalignment and mode mixity calculations

After insertion, the pin's geometry and the final state (or form) of a pin within the laminate will vary, as has been seen from the UAZ process in [10]. It is expected that there would still be some variation even for the more controlled manual insertion used and so each specimen was inspected using X-ray CT in order to identify the exact condition of the pin inside the laminate including form, misalignment from the intended surface normal orientation and any damage which may have occurred. Examples of typical pin conditions are shown in Figure 3.

(*Insert figure 3*)

(*Insert figure 4)*

The individual pin misalignment angle was measured to assess the exact orientation in the specimen and to understand the statistical distribution for the entire manufactured batch. The axis system and the label conventions of the misalignment angles are presented in Figure 4. The relative offset angle from the vertical (z-axis), ζ, and the deviation from the 0° fibre direction (x-axis), Ψ, of each pin are calculated from the misalignment angles, α13 and α23 using the following expressions:

$$\tan\zeta = \sqrt{\tan^2\alpha_{13} + \tan^2\alpha_{23}} \quad (1)$$

$$\tan\psi = \frac{\tan\alpha_{23}}{\tan\alpha_{13}} \quad (2)$$

Approximately 60 samples were manufactured for each configuration with the population of the relative pin offset angles (ζ), presented in Figure 5. The distribution of offset angles follows a standard distribution bell curve with a mean value of 13°±7.5 for UD and 13.5°±4.5 for the QI specimens. Readers should note that the calculated average misalignment corresponds to the manual insertion process used for this study and is not necessarily representative of the traditional UAZ insertion process.

For the experimental tests, specimens were selected such that the pins did not exhibit visible defects such as those shown in (Figure 3 a-c) and misalignment angles of less than 20° from vertical (ζ). The decision to use this angle as our selection criterion was based on the number of samples we could realistically acquire to give a suitable amount to test as well as ensuring that we were covering the full range of insertion angles reported in the literature.

(*Insert figure 5*)

To apply a mixed mode through-thickness loading varying from pure mode I to pure mode II, each specimen was rotated in the zx plane by an angle, χ, relative to the loading direction, P, as shown in Figure 4b. The specimen rotation alone cannot define the correct load mode mixity of the pins in the xy plane when pin misalignment is present. Therefore, the loading mode mixity was calculated for each specimen taking into account the pin offset angle (ζ), deviation from x-axis (ψ) and the rotation of the specimen or nominal mixed mode angle (χ) relative to the loading direction. The total force acting on the pin ($\overline{N}$) can be resolved in terms of the pin axis as:

$$\overline{N} = \begin{bmatrix} N_z \\ N_x \\ N_y \end{bmatrix} = \begin{bmatrix} \sin\zeta\cos\psi & \sin\zeta\sin\psi & \cos\zeta \\ \cos\zeta\cos\psi & \cos\zeta\sin\psi & -\sin\zeta \\ -\sin\psi & \cos\psi & 0 \end{bmatrix} \begin{bmatrix} P\sin\chi \\ 0 \\ P\cos\chi \end{bmatrix} \tag{3}$$

Where N_z is the axial load and N_x and N_y are the shear loads acting on the pin. By taking the load mode mixity (ϕ) as the ratio of the shear loads to the total load:

$$\phi = \sqrt{\frac{{N_x}^2 + {N_y}^2}{{N_z}^2 + {N_x}^2 + {N_y}^2}} \tag{4}$$

The load mode mixity then reduces to:

$$\phi = \sqrt{\cos^2\chi\sin^2\zeta + \sin^2\chi\left(\sin^2\psi + \cos^2\psi\cos^2\zeta\right) - \frac{1}{2}\sin 2\chi\sin 2\zeta\cos\psi} \tag{5}$$

The corrected mixed mode angle (ω) can then be calculated using:

$$\omega = \tan^{-1}\left(\frac{\phi}{\sqrt{1-\phi^2}}\right) \tag{6}$$

Note that for the case where there is no misalignment, i.e. when ζ and ψ are 0° then ω will be equal to the nominal mixed mode angle χ.

4. Test Setup

All the experimental tests were carried out using a calibrated 1kN load cell and bespoke fixtures designed and manufactured at the University of Bristol. The mode I and mixed mode tests were carried out using the mixed mode test fixture (Figure 6). This fixture comprises of a top and bottom section, each of which is coupled to the upper and lower crossheads of the testing machine, respectively. The central rotating plate is split into two, with a cut-out to accommodate the 20 × 20 × 8 mm test specimen. To attach the specimen to the fixture, a small amount of cyanoacrylate superglue (Loctite Corp., UK) was applied on each corner of the specimen, taking care to ensure that the glue did not spread to contact the pin. Individual specimens were then located into the cut-out with the 0° fibre direction being perpendicular to the plane of the test fixture. The plate was then rotated between 0° (Mode I) and 90° (Mode II) in 15° intervals to achieve the desired mixed mode angle. Once in position the rotating plate was secured to the top and bottom parts of the fixture with standard cap screws. Unless otherwise stated all samples were loaded such that the nominal rotation (χ) was made about the y-axis of the specimen (Figure 4).

(*Insert figure 6*)

The mode II shear testing fixture shown in Figure 7 comprises of two inner blocks which hold the test specimen and were designed to slide parallel to each other, shearing the top and bottom half of the specimen. The blocks fit inside a rigid outer guide which was included to prevent any out of plane opening. To reduce the contact area between the inner blocks and the outer guide, and hence the friction induced as they slide past each other, raised, semi-circular profiles were incorporated into the design. The upper and lower fixture parts are pin jointed and free to rotate when not constrained by the outer guide. While sliding, the mass of the fixtures may result in an

opening moment to the test specimen. To minimise this, the fixture was designed such that the centre of gravity of the blocks are aligned with the loading line of the test machine. All of the test specimens were positioned such that the pins were 'with the nap' to the loading direction (Figure 1). It is important to note that for the UD laminate types, the specimen can be set up such that the mode II loading direction can drive the pins either in between the fibres into the resin pocket (soft direction) or into the fibres running transverse to the direction of loading (hard direction). For this reason, the UD specimens in the pure mode II were loaded in both the soft and the hard direction to assess the response of pins. For all the mixed mode cases the specimens where orientated such the mode II component of the load was in the 'soft direction'. The opening and sliding displacements were measured on all the samples using a non-contact video extensometer (Imetrum Ltd. [18]). It must be noted that it was not possible to achieve precisely pure mode II conditions even when out of plane opening is constrained. It was found that there was on average a 0.08mm±0.03 opening during the mode II tests as measured using a non-contact video extensometer.

(*Insert figure 7*)

Displacement was applied to the specimen at a rate of 0.5 mm/min until the pin failed, either by fracture or complete pull-out from the laminate.

5. Results and Discussions

For each test specimen, load vs. displacement plots were obtained. Representative curves from the each sample undergoing nominal rotations (χ) from 0° to 90°, for the UD and the QI specimens are shown in Figure 8 and Figure 9.

(*Insert figure 8*)

(*Insert figure 9*)

From initial observations it appears for there to be a non-monotonic trend in the curves with increase in the nominal rotation of the samples. This variability is caused by inherent inconsistencies in individual pin quality, manufacturing variances and specimen handling during the test procedures. Although great care was adopted to reduce any variability, it was not possible to get a high degree of control on some of these issues. For this reason it is not possible to make quantitative examinations from these plots. Further analysis will be made to assess the 'absorbed' energy relative to corrected mixed mode angle (ω).There is a clear difference in the mode I pull-out response of the pins in the UD specimens compared to the QI type. The two stages of the pin pull-out response are shown in Figure 10. These stages have been termed tri-linear mode I bridging traction [9]. In stage I, the response is the result of the pin bond strength with the matrix resin. For the UD laminates the maximum load required to overcome this bonding strength was on average 86N ±5. For the QI configuration it was not possible to distinguish such debond load as the load response between debond and frictional pull-out was constantly smooth. In stage II the response is dominated by the frictional pull-out of the pins from the laminate. A higher load is exhibited by the UD laminates compared to the QI laminates in stage II also.

The difference in response between the UD and QI type specimens can be attributed to the difference in thermal contraction of the laminate and the pins during the cooling down process following cure [12]. In the UD case there are no off angle plies which would inhibit the thermal contraction in the transverse direction of the laminate. Thus the laminate will be unrestrained to contract in the transverse direction and not disbond from the pin. However, in the QI case the presence of the multiple ply orientations inhibits the contraction of the laminate in these respective fibre directions. For this reason, the pin, when contracting during the cool down from the

laminate cure temperature, will develop significant residual stresses at its boundary with the laminate, weakening the pin/matrix interface. This reduces or even eliminates stage I of the bridging mechanism for the QI case. Thus only stage II, frictional pull-out of the pins was observed, as seen in some of the curves. Attempts were made to examine whether any interfacial cracking had developed as a result of thermal mismatch contractions, however from external observation through optical microscopy, it was not possible to deduce whether any minor cracking observed was the result of the thermal contractions or other factors. It remains to be seen whether any cracking is present around the entrenched body of the pin.

(*Insert figure 10*)

At higher loading mode mixities, the UD type specimens did not exhibit pull-out. This is due to the combination of the bond strength between the pin and the matrix and the enhanced friction due to the rotated pin acting on the foundation of the composite, this enhancement is termed ‘snubbing’ and is analysed in great detail by Cox [14]. The load necessary to overcome this exceeds the rupture limit of the pin.

The QI type specimens exhibit pull-out up to higher mode II mixities than the UD type specimens. The increased friction due to the lateral loading of the misaligned pin at the pin/matrix interface results in higher peak work than those with lower misalignment angle. At higher mode mixities the force required to overcome the increased friction eventually exceeds the pin rupture limit, thus partial pull-out was observed prior to rupture of the pin in bending. SEM micrographs of the tested samples are shown in Figure 11. In mode I the pins completely pull out of the composite with little or no damage (Figure 11 a). At higher mode mixities the deflection of the pins initially causes longitudinal splits inside the pins before final failure (Figure 11 b). In pure mode II loading, very little to no pull-out was observed

which resulted in a confined bending failure of the pins that appears almost similar to shear failure for both the UD and the QI configurations (Figure 11 c). It is evident that the failure mechanism of the pins is complicated. When loaded in mixed mode conditions the pin may reach a rupture limit. This limit could be either the result of bending, tensile or shear failure of the pin or a combination of the three, thus a simple strength calculations cannot be used to reliably predict the failure loads of the pins.

(*Insert figure 11*)

There is no succinct way of including all the load plots for each sample within the context of this paper. Reporting the peak loads for each samples may be misleading, since peak loads may correspond to the maximum frictional force, pin debonding strength or rupture limit of the pins. For this reason it was chosen to summarise the results using energy plots as these encapsulate peak loads, frictional pull-out and de-bonding.

For each specimen, the energy required to pull-out and/or rupture the pin, W, was calculated by integrating the load versus displacement curves between the origin until complete pull-out or rupture, Figure 10. The plots of energy against the corrected mixed mode angle (ω) from the loading direction for the UD and the QI laminates are shown in Figure 12 and Figure 13. Both laminate types exhibit a transition region between pull-out and rupture failure, as marked on the plots. This transition region is bounded by the minimum angle at which a pin ruptured during the testing and a maximum angle at which a pin exhibited complete pull-out. The minimum corrected mixed mode angle that a pin in a UD laminate ruptured is relatively low; approximately 11° compared to 33° in the QI laminates.

There is a large scatter in the energy for pulled-out pins in the QI samples. A strong relationship between increase in mixed mode angle (equation 6) and pull-out energy

(Figure 13) would be expected due to the enhancement of the friction caused by the lateral loading of the rotated pin at the pin/matrix interface. However, from the results this relationship appears to be a weak one and this is due to high level of inserted pin quality variance, which is the source of the large scatter.

For both the UD and QI samples there is a sharp drop in energy in the transition region, indicative of a small number of samples rupturing during pull-out. In the rupture region, the scatter in the data is reduced and all the samples show similar failure energies.

(*Insert figure 12*)

(*Insert figure 13*)

For the UD laminates, the samples that were loaded in the hard direction (pins loaded against the 0° fibres) are circled. From the limited number of samples loaded in both hard and soft direction in pure mode II, it was observed that they showed very similar responses. One could perhaps argue that for the samples loaded in the hard direction, the failure energies are uniformly lower than those in the soft direction. This may be due to a stiffer response of the laminate triggering failure at lower displacements. However more data would be needed to make definitive conclusions.

6. Conclusions

A significant body of experimental data has been generated which has characterised the behaviour of pin reinforcements over the full range of mode mixities. This has allowed trends and generic behaviour to be identified which can be helpful in understanding the overall performance of pin reinforcement at structural level and how it can be used best in design to overcome delamination problems.

It was confirmed that the bridging mechanism in mode I and some mixed mode loading cases develops over two stages (Figure 10). Stage I depending on the pin/matrix interface strength whilst Stage II involving the frictional pull-out of the pins from the laminate.

Laminate stacking sequence has a direct influence on the pin pull-out behaviour in mode I and in some lower mode I/II mixities. UD laminates experience far greater transverse contraction during the cooling down process following cure than non-UD laminate types, which results in superior pin/matrix bond strength as well as increased surface friction of the pin during the pull-out stage. For this reason pins inside the UD samples ruptured at lower mixed mode angles than the QI specimens.

Stacking sequence appears to have no influence on pin behaviour at mode mixities approaching pure mode II. In both UD and QI samples, the pins are restricted to pull out and thus rupture with failure energies similar to those close to pure mode II.

From the data produced in this study it was possible to create maps of bridging energy versus mixed mode loading angle. This revealed a clear transition in behaviour from pull-out to pin rupture over a relatively small angle change.

At the higher level of detail, the single pin response data is an essential requirement for the effective development and calibration of pin bridging laws, which can be implemented subsequently into a cohesive zone models for high fidelity finite element analysis [19].

7. Acknowledgements

The authors would like to acknowledge Rolls-Royce plc for their support of this research through the Composites University Technology Centre (UTC) at the

University of Bristol, UK and Daniel Thompson for his preparation and testing of some of the specimens.

8. References

[1] Velmurugan R, Solaimurugan S. "Improvements in Mode I interlaminar fracture toughness and in-plane mechanical properties of stitched glass/polyester composites," *Composites Science and Technology*, vol. 67, no. 1, pp. 61–69, 2007.

[2] Cartié DDR, Dell'Anno G, Poulin E, Partridge IK. "3D reinforcement of stiffener-to-skin T-joints by Z-pinning and tufting," *Engineering Fracture Mechanics*, vol. 73, no. 16, pp. 2532–2540, Nov. 2006.

[3] Partridge IK, Cartie DDR. "Delamination resistant laminates by Z-Fiber pinning: Part I manufacture and fracture performance," *Composites Part A: Applied Science and Manufacturing*, vol. 36, no. 1, pp. 55–64, 2005.

[4] Zhang X, Hounslow L, Grassi M. "Improvement of low-velocity impact and compression-after-impact performance by z-fibre pinning," *Composites Science and Technology*, vol. 66, no. 15, pp. 2785–2794, 2006.

[5] Rugg KL, Cox BN, Massabò R. "Mixed mode delamination of polymer composite laminates reinforced through the thickness by z-fibers," *Composites Part A: applied science and*, vol. 33, pp. 177–190, 2002.

[6] Koh TM, Feih S, Mouritz AP. "Experimental determination of the structural properties and strengthening mechanisms of z-pinned composite T-joints," *Composite Structures*, vol. 93, no. 9, pp. 2222–2230, 2011.

[7] Cartie DDR, Troulis M, Partridge IK. "Delamination of Z-pinned carbon fibre reinforced laminates," *Composites Science and Technology*, vol. 66, pp. 855–861, 2006.

[8] Liu H, Yan W, Yu X, Mai Y. "Experimental study on effect of loading rate on mode I delamination of z-pin reinforced laminates," *Composites Science and Technology*, vol. 67, no. 7–8, pp. 1294–1301, Jun. 2007.

[9] Mouritz AP, Koh TM. "Re-evaluation of mode I bridging traction modelling for z-pinned laminates based on experimental analysis," *Composites Part B*, vol. 56, pp. 797–807, 2014.

[10] Chang P, Mouritz AP, Cox BN. "Properties and failure mechanisms of z-pinned laminates in monotonic and cyclic tension," *Composites Part A: Applied Science and Manufacturing*, vol. 37, no. 10, pp. 1501–1513, Oct. 2006.

[11] Cartié DDR, Cox BN, Fleck NA. "Mechanisms of crack bridging by composite and metallic rods," *Composites Part A: Applied Science and Manufacturing*, vol. 35, no. 11, pp. 1325–1336, Nov. 2004.

[12] Sweeting RD, Thomson RS. "The effect of thermal mismatch on Z-pinned laminated composite structures," *Composite structures*, vol. 66, pp. 189–195, 2004.

[13] Cox B, Sridhar N. "A traction law for inclined fiber tows bridging mixed-mode cracks," *Mechanics of Advanced Materials and Structures*, no. 9, pp. 299–331, 2002.

[14] Cox BN. "Snubbing Effects in the Pullout of a Fibrous Rod from a Laminate," *Mechanics of Advanced Materials and Structures*, vol. 12, no. 2, pp. 85–98, Mar. 2005.

[15] Allegri G, Zhang X. "On the delamination and debond suppression in structural joints by Z-fibre pinning," *Composites Part A: Applied Science and Manufacturing*, vol. 38, no. 4, pp. 1107–1115, Apr. 2007.

[16] Zheng XT, Gou LH, Han SY, Yang F. "Experimental and Numerical Study on the Mode I Delamination Toughness of Z-Pinned Composite Laminates," *Key Engineering Materials*, vol. 417–418, pp. 185–188, Oct. 2009.

[17] Bianchi F, Zhang X. "A cohesive zone model for predicting delamination suppression in z-pinned laminates," *Composites Science and Technology*, vol. 71, no. 16, pp. 1898–1907, Nov. 2011.

[18] "Imetrum Limited," 2014. [Online]. Available: http://www.imetrum.com. [Accessed: 10-Jan-2014].

[19] Mohamed G, Helenon F, Allegri G, Yasaee M, Hallett SR. "Predicting the through-thickness enhancement of z-pinned composite laminates," in *19th International Conference on Composite Materials*, Montreal, Canada, 2013.

Figures

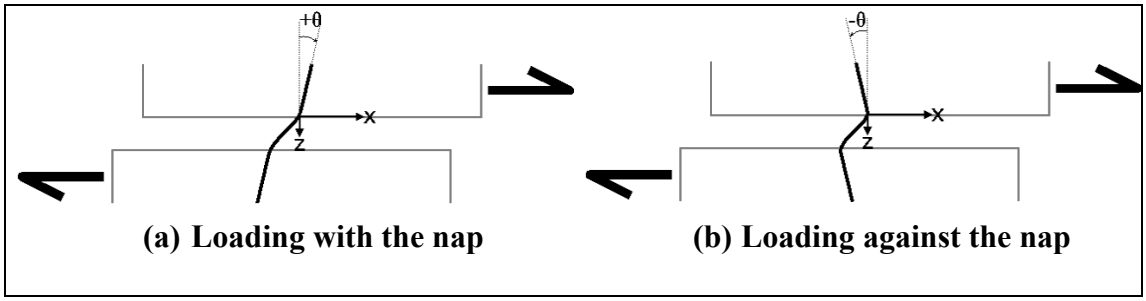

Figure 1 Pin orientation relative to the pure mode II loading direction (a) If angle θ is positive, load is with the nap (b) If angle θ is negative, load is against the nap

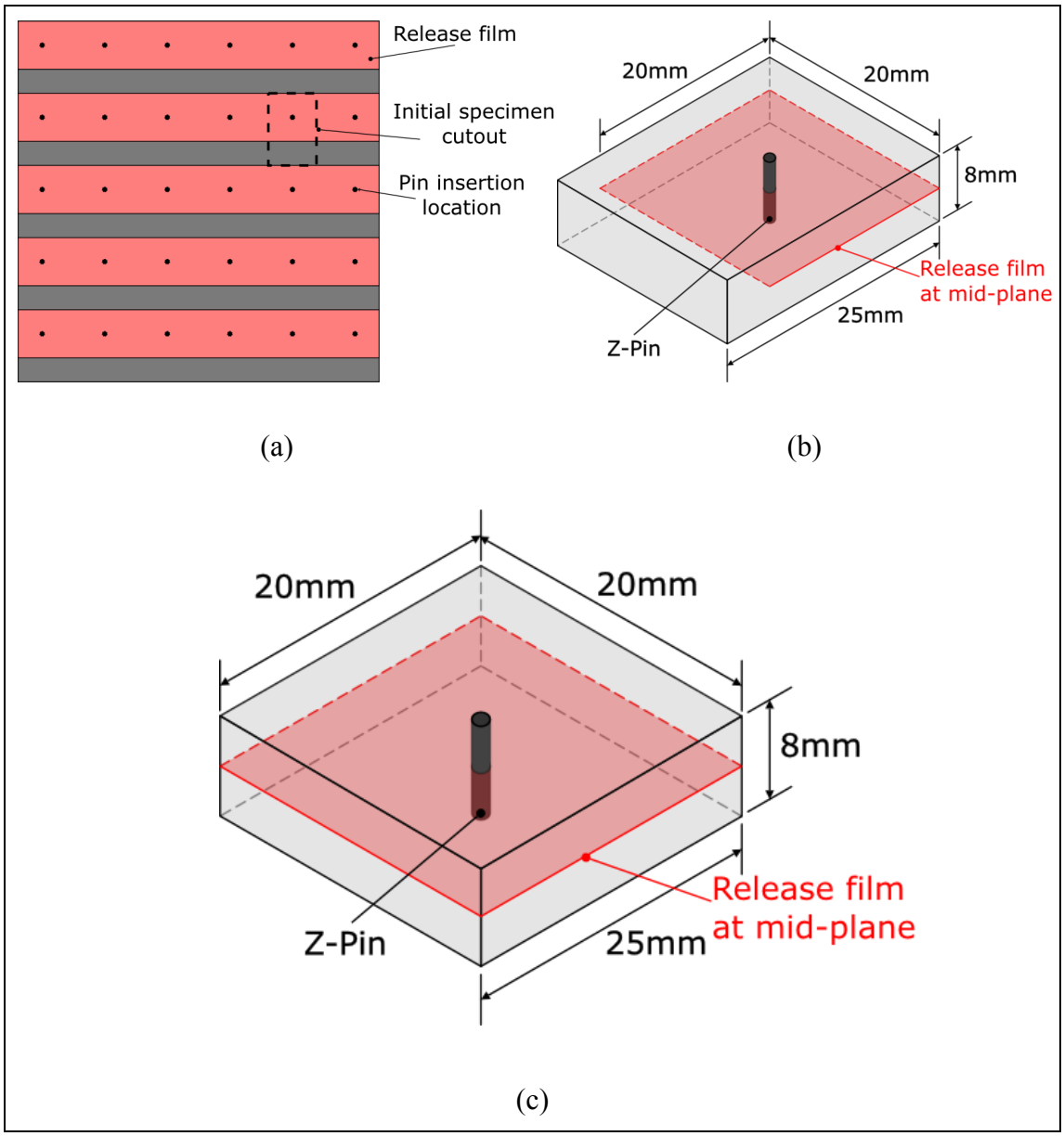

Figure 2 (a) Laminated plate with release film inserts at mid-plane (b) Initial machined specimen with 5mm bonded region for safe handling (c) Final machined specimen dimensions before testing

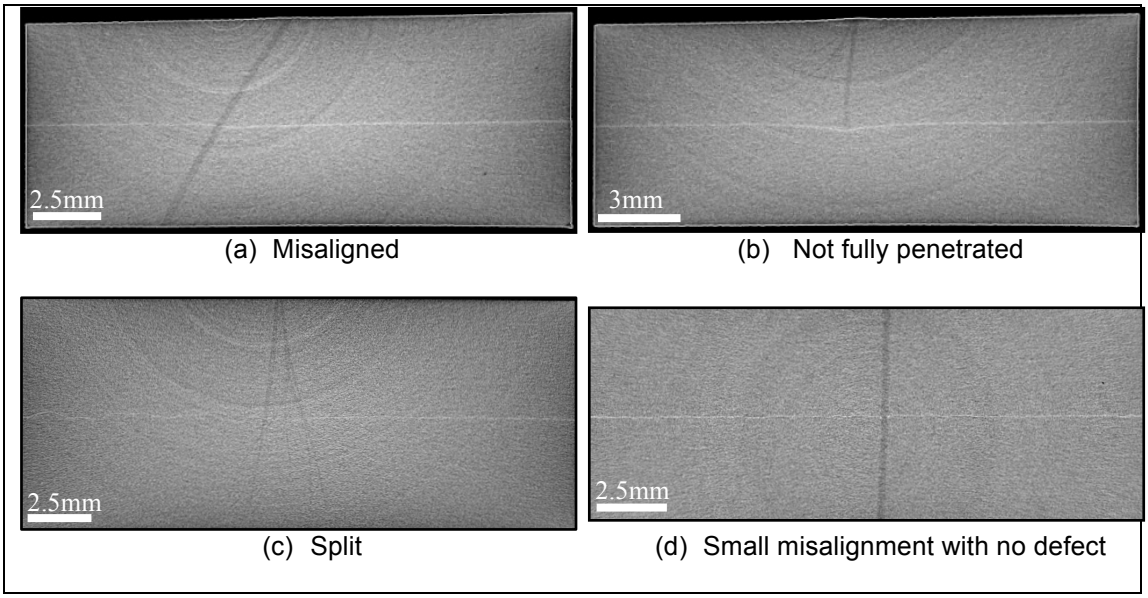

Figure 3 X-ray CT scan slices showing examples of typical pin condition following the manufacturing process

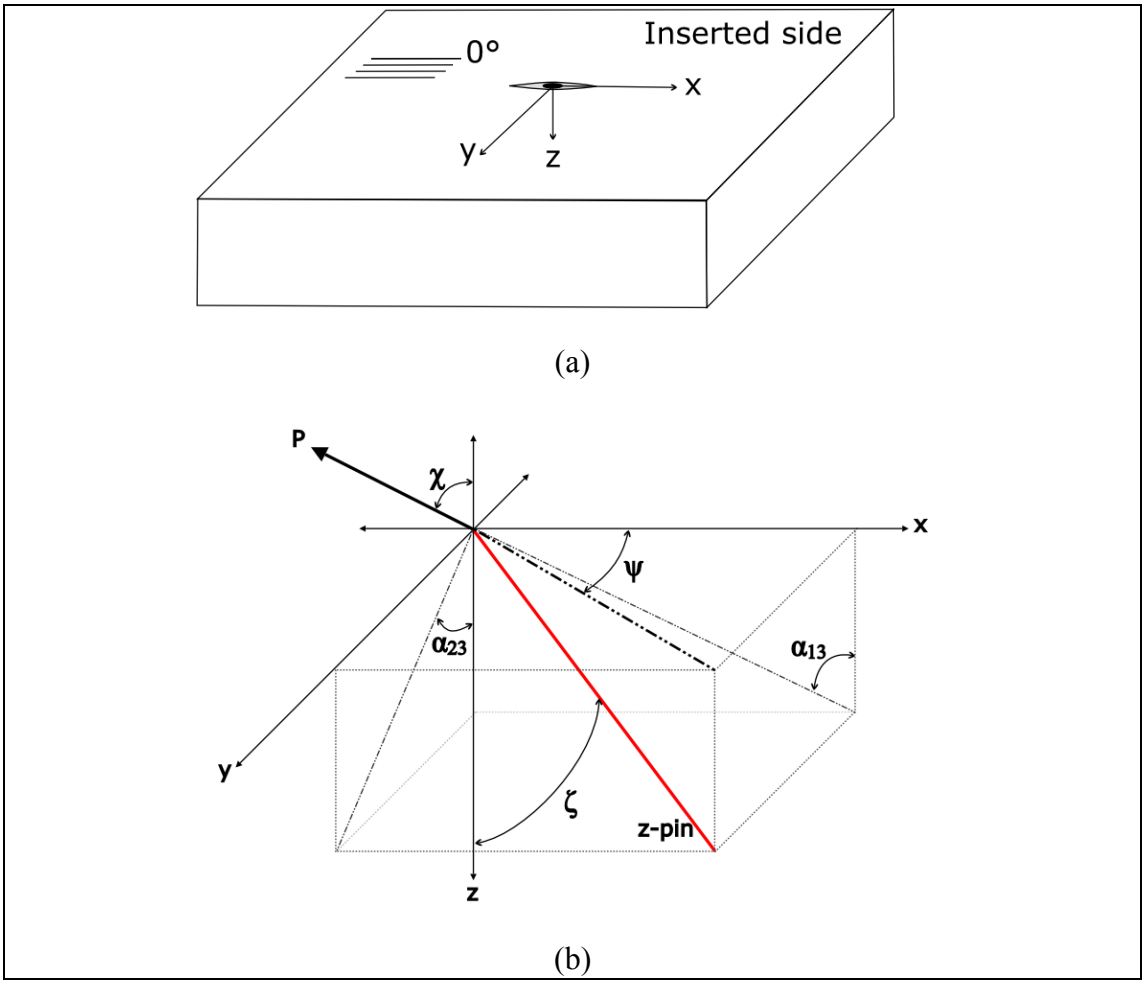

Figure 4 (a) Composite axis system (b) Pin alignment angle labelling convention

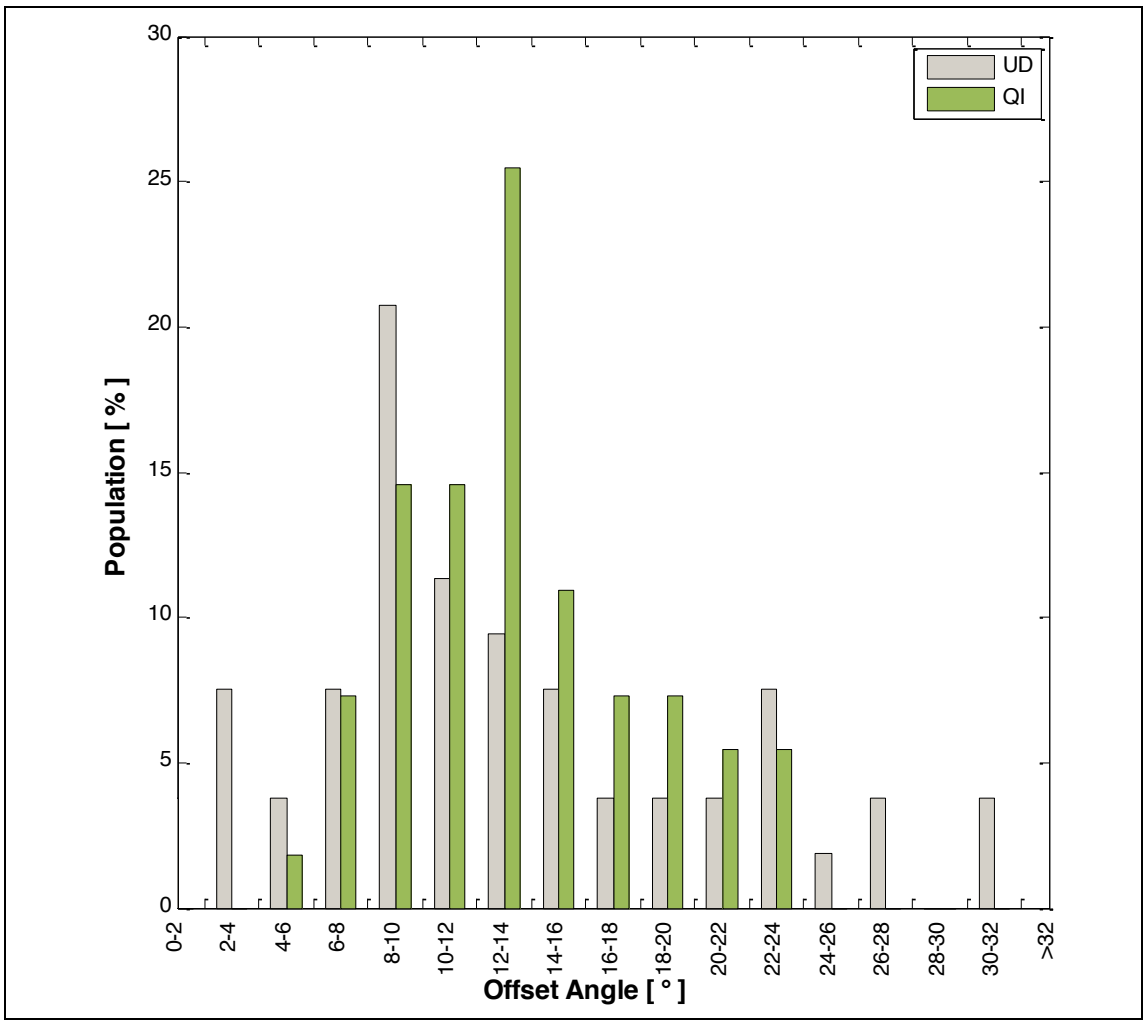

Figure 5 Population of pin offset angle (ζ) after the manufacturing process

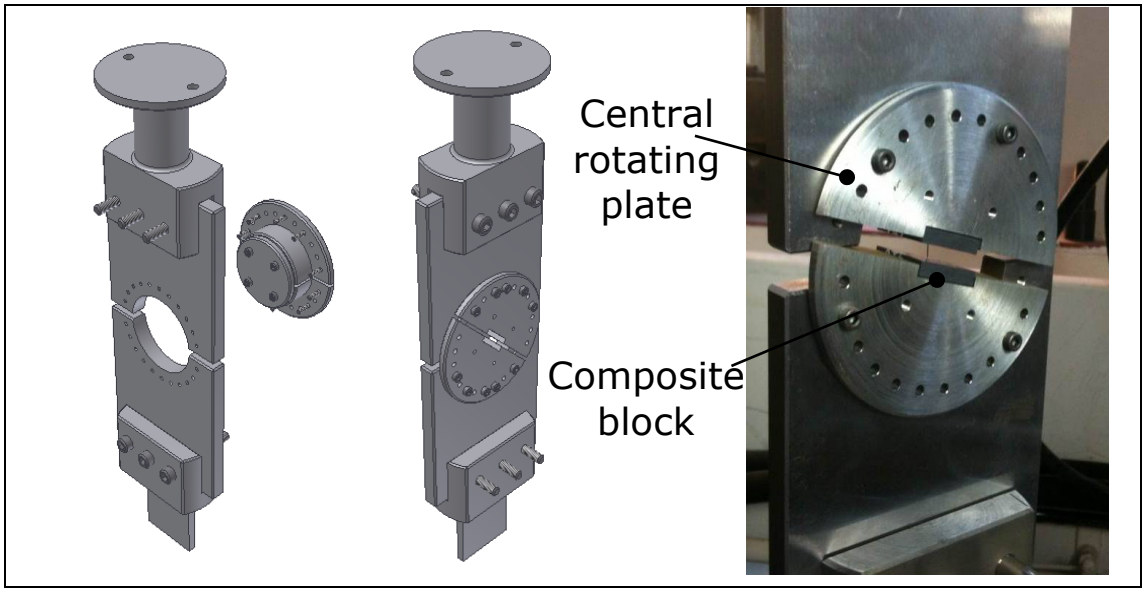

Figure 6 Fixture for the mixed mode I/II testing

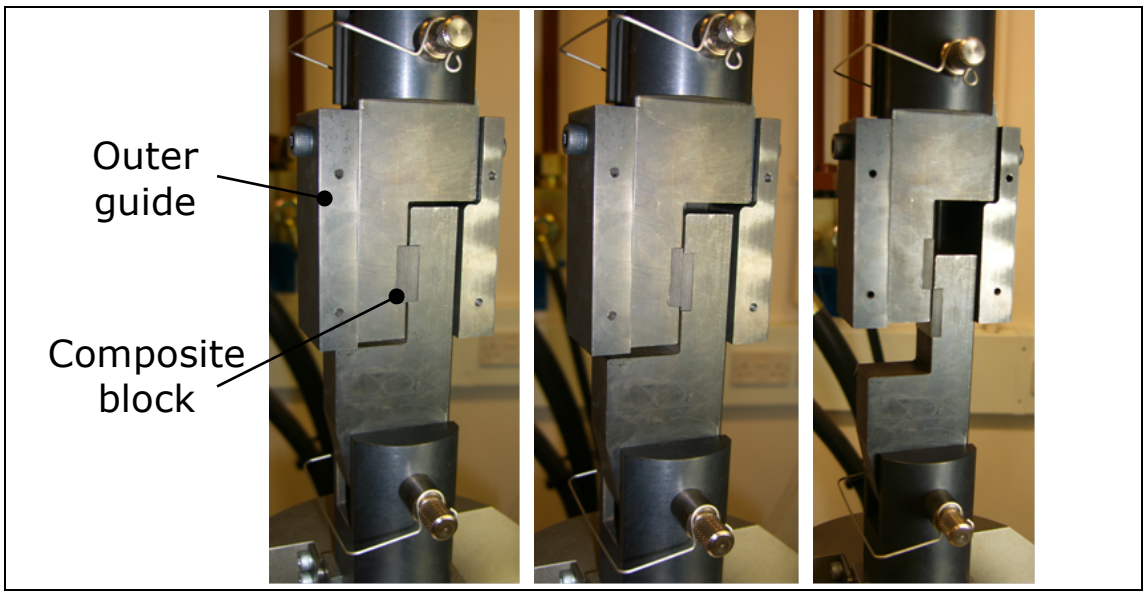

Figure 7 Fixture for the mode II shear testing, highlighting the movement of the loading blocks inside the outer guide and the relative sample position

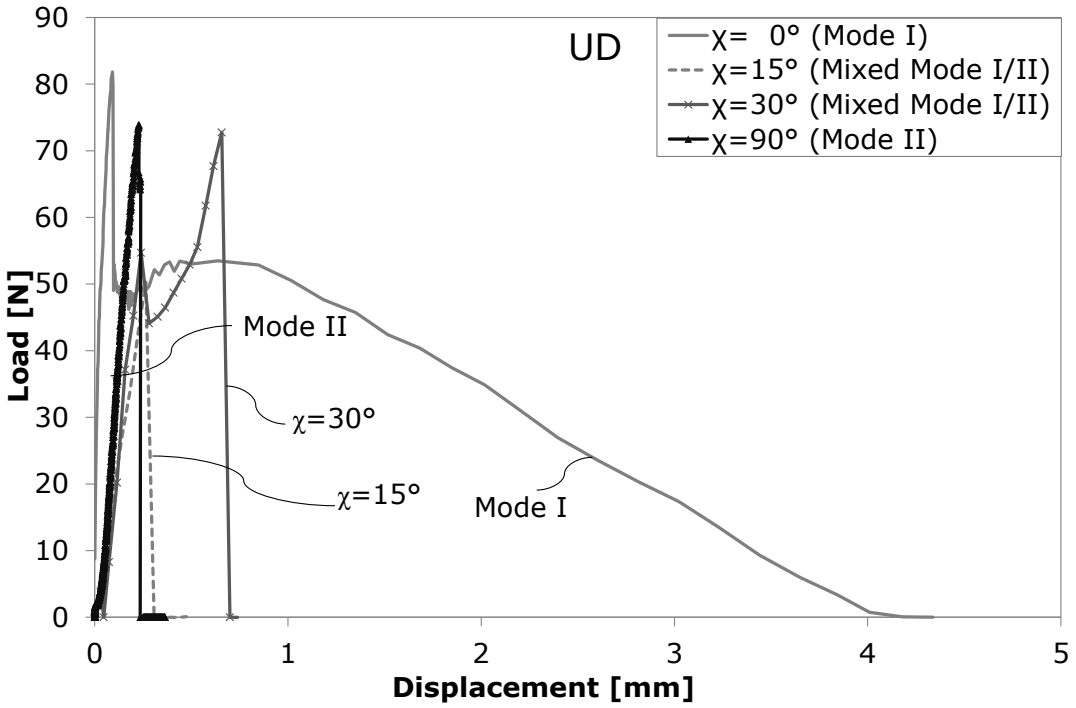

Figure 8 Representative UD laminate load vs. displacement results (Mixed mode and mode II curves from sample loaded in 'soft' direction)

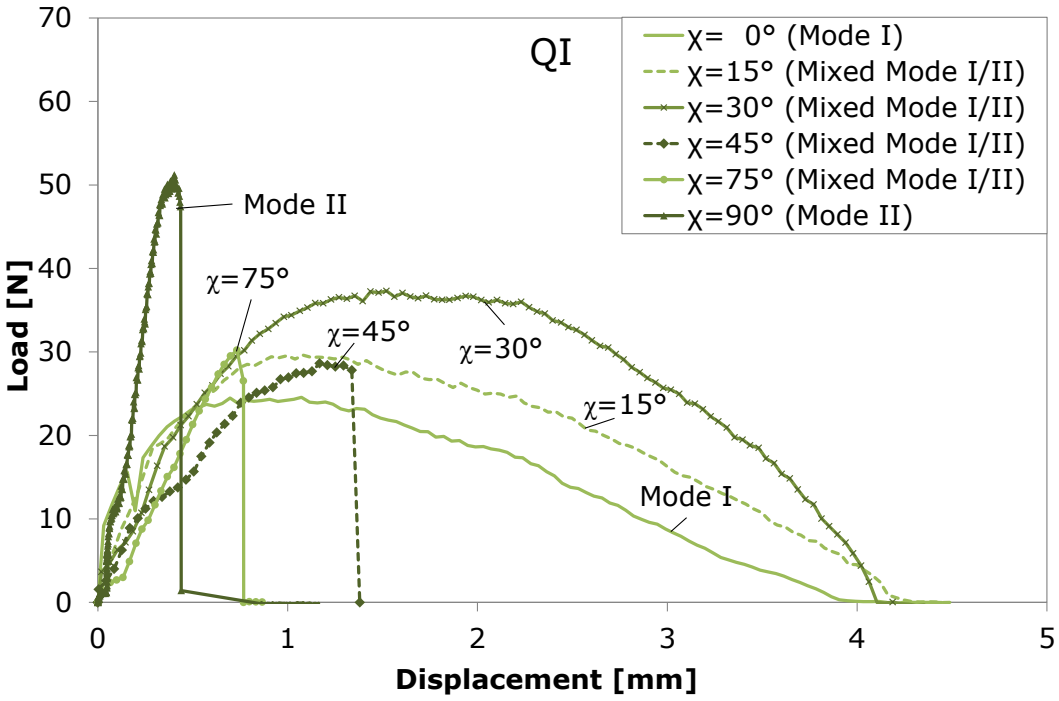

Figure 9 Representative QI laminate load vs. displacement results

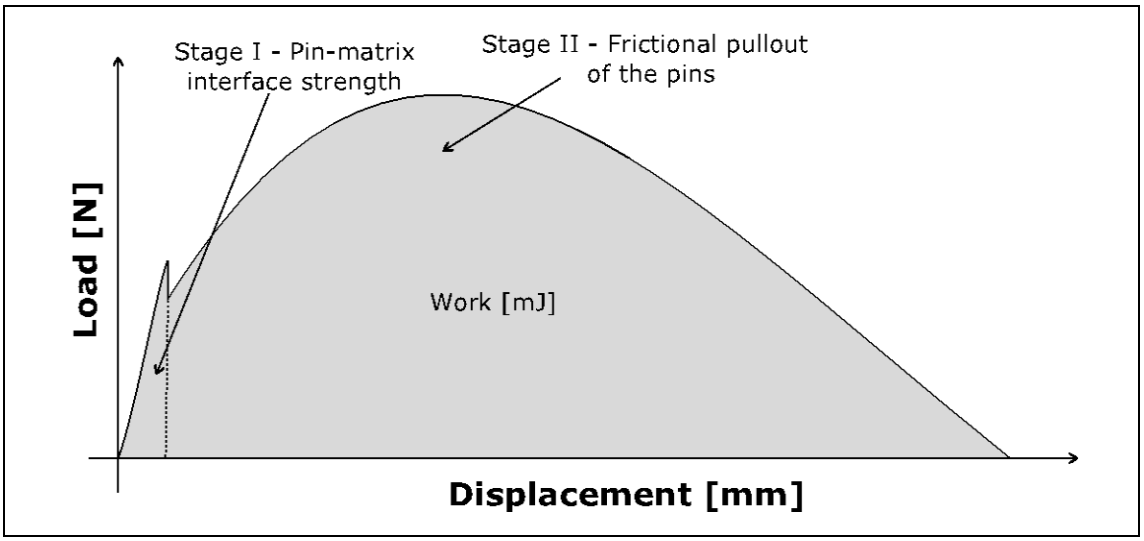

Figure 10 Two stage bridging mechanism in mode I and some mixed mode I/II cases

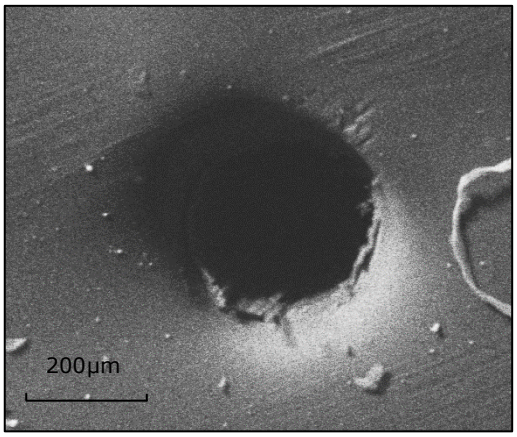

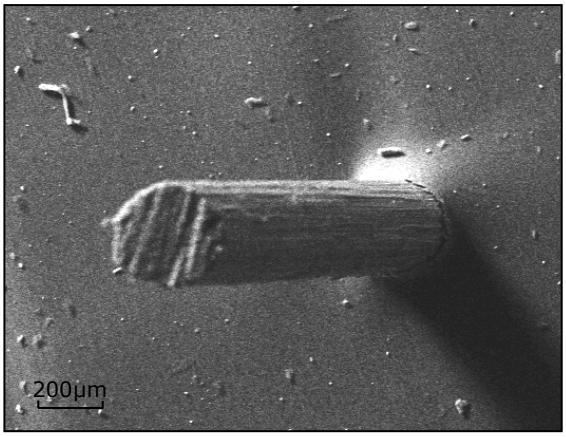

(a) Undamaged single z-pin pull-out in mode I

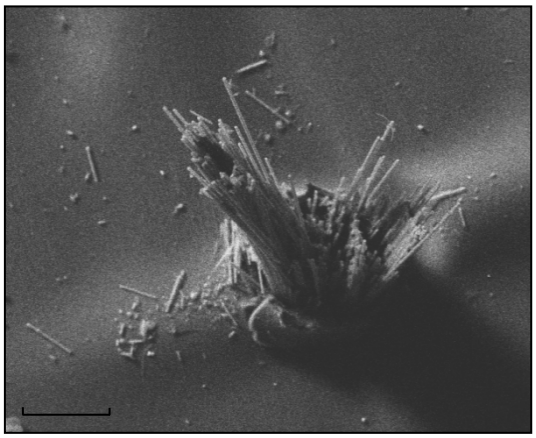

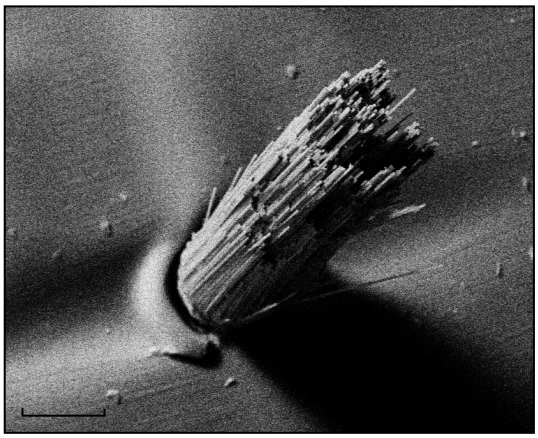

(b) Longitudinal pin splitting and eventual pin failure in bending of mixed mode tests

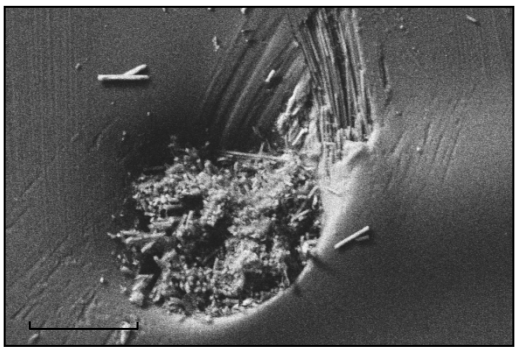

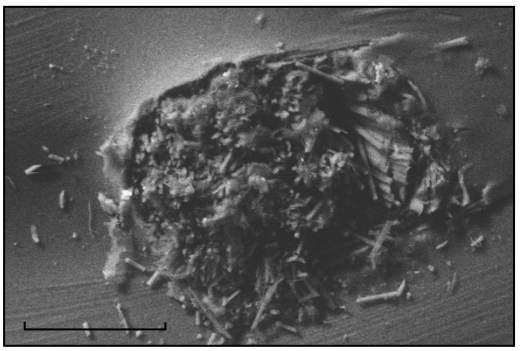

(c) Pin shear failure in in pure mode II tests

Figure 11 SEM micrographs of carbon composite pin after (a) mode I (b) mixed mode (c) mode II tests (Left and right images are bottom and top surfaces respectively)

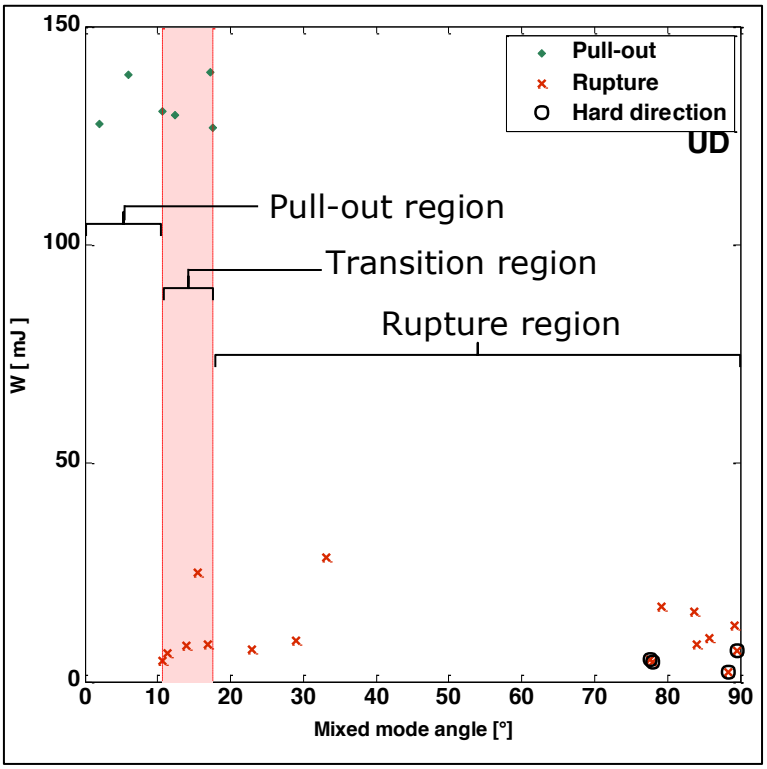

Figure 12 Absorbed energy vs. corrected mixed mode angle for failure/pull-out of pins inside UD laminates

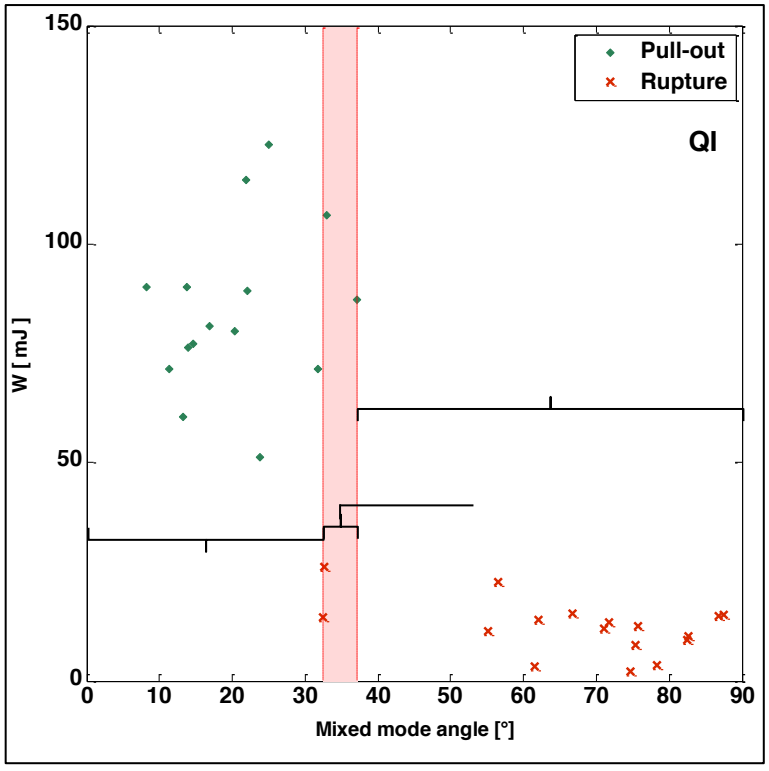

Figure 13 Absorbed energy vs. corrected mixed mode angle for failure/pull-out of pins inside QI laminates